Journal of Magnetism and Magnetic Materials 561 (2022) 169671

Contents lists available at ScienceDirect

Journal of Magnetism and Magnetic Materials

journal homepage: www.elsevier.com/locate/jmmm

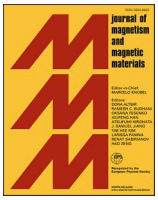

Measurement and analysis of the non-symmetry of transverse magnetisation and resulting loss in grain-oriented steel using a modified RSST

Shuaichao Yue [a,b], Anthony J. Moses [a,*], Philip I. Anderson [a], Christopher Harrison [a], Yongjian Li [b], Qingxin Yang [b]

[a] School of Engineering, Cardiff University, Cardiff CF24 3AA, United Kingdom
[b] State Key Laboratory of Reliability and Intelligence of Electrical Equipment, Hebei University of Technology, 300130 Tianjin, China

ARTICLE INFO

Keywords:
Magnetic measurement
Anisotropy
Rotational single-sheet tester (RSST)
Electrical steels

ABSTRACT

A modified rotational single-sheet tester, in which a circular sample can be rotated to be magnetised along arbitrary directions, was used to study the transverse magnetisation and associated losses in grain-oriented electrical steel (GOES).

Longitudinal and transverse components of flux density B and magnetic field H in a sample of commercial GOES were measured under alternating excitation at angles from −90° to +90° to the rolling direction (RD) at peak flux densities up to 1.5 T over a magnetising frequency range of 20–400 Hz. The loss due to the transverse components of B and H, referred to as the transverse loss, was evaluated.

At 1.5 T, 20 Hz, the transverse loss was less than 0.1 mW/kg when magnetised along either the RD or the transverse direction but it rose to around 5 mW/kg when magnetised at 30° to the RD. It was found to be magnetising direction, frequency and flux density dependent. The transverse loss was a simple function of the angle of magnetisation with respect to the RD but it differed when magnetised along directions on either side of to the RD dependent on the grain structure in the measurement region.

The basic phenomenon is explained with the aid of simple magnetic domain and magnetisation models. The difficulty of quantifying its absolute effect in GOES and non-oriented electrical steel is discussed. It appears that transverse magnetisation in GOES is not normally large enough to have any practical effect on measurements obtained using IEC Standard loss testers or on the prediction of electrical machine core losses.

A preliminary series of tests showed that transverse loss also occurs in non-oriented electrical steel but it is difficult to quantify.

1. Introduction

Grain-oriented electrical steel (GOES) is widely used in power transformer and large generator cores. Knowledge of its magnetisation characteristics and losses are necessary in the development and application of effective models for predicting their magnetic performance.

Magnetic properties of GOES are usually characterised using the well-established Epstein Square or a single sheet tester (SST) [1]. These are used by steel producers and users to compare the losses and permeabilities of electrical steel laminations magnetised along fixed directions, usually the rolling direction (RD) and sometimes the transverse direction (TD). They only respond to components of magnetic flux and surface fields parallel to the applied field direction which limits their ability to measure the total loss in the steel as will be apparent later.

Components of flux at angles to the magnetising direction occur during rotational magnetisation which can be predominant in the joints of multi-phase transformer cores and rotating machine stator cores. Transformer designers often predict the localised rotational losses in a core and incorporate it into the Building Factor (BF) [2].

Several groups have designed rotational single-sheet testers (RSSTs) to measure characteristics of electrical steel under controlled rotational magnetisation. These are well documented, (e.g. see [3–5]), although until now, there is no international standard for RSST topologies or the measurement protocol.

The main aim of this investigation was to quantify small components

* Corresponding author.
E-mail address: Mosesaj@cf.ac.uk (A.J. Moses).

https://doi.org/10.1016/j.jmmm.2022.169671
Received 11 May 2022; Received in revised form 29 June 2022; Accepted 29 June 2022
Available online 8 July 2022

nomenclature

b	Distance between a pair of B-needles
$\boldsymbol{B}$	Magnetic flux density
BF	Building factor
B_x	Longitudinal component of flux density
B_y	Transverse component of flux density
B_{xp}	Amplitude of longitudinal component of flux density
B_{xrms}	RMS value of longitudinal magnetic flux density
B_{yrms}	RMS of transverse magnetic flux density
d	Sample thickness
f	Excitation frequency
GOES	Grain-oriented electrical steel
$\boldsymbol{H}$	Magnetic field strength
$\boldsymbol{H_d}$	Demagnetising magnetic field
$\boldsymbol{H_{ex}}$	Applied magnetic field
H_x	Longitudinal magnetic field strength
H_y	Transverse magnetic field strength
H_{xrms}	RMS value of longitudinal magnetic field strength
H_{yrms}	RMS value of transverse magnetic field strength
J_s	Saturation polarisation
K_{hx}	Coil coefficient of x-axis H-coil
K_{hy}	Coil coefficient of y-axis H-coil
M	Magnetisation
NO	Non-oriented
P_x	Loss due to longitudinal components of $\boldsymbol{B}$ and $\boldsymbol{H}$
P_y	Loss due to transverse components of $\boldsymbol{B}$ and $\boldsymbol{H}$
P_t	Total loss
RD	Rolling direction
RSST	Rotational single-sheet tester
SST	Single-sheet tester
T	Time period of excitation
TD	Direction 90° to the RD
V_{bx}	Instantaneous voltage across x-axis B-needles
V_{by}	Instantaneous voltage across y-axis B-needles
V_{hx}	Instantaneous voltage across x-axis H-coil
V_{hy}	Instantaneous voltage across y-axis H-coil
k	Transverse loss coefficient
(x) axis	Longitudinal direction
(y) axis	Transverse direction
α	Yaw angle of misaligned grain
β	Angle between $\boldsymbol{H}$ and (x) axis
ρ	Mass density
θ	Angle between $\boldsymbol{H_{ex}}$ and the RD
μ_0	The magnetic constant

of transverse field and flux density when a sample of GOES was magnetised at fixed angles to its RD. A sensitive and versatile test system was designed to carry out the measurements.

This paper gives a brief explanation of the origin of transverse flux and the associated loss in mis-oriented grains in GOES sheet. This is followed by an explanation for choosing what we refer to as the Modified RSST for our measurements and an outline of its design and operation. Transverse magnetisation and loss characteristics of a GOES are presented together with an analytical model showing the cause of the phenomenon and quantifying its magnitude in commercial GOES for the first time.

2. Transverse flux and loss in mis-oriented grains

GOES is highly anisotropic due to a strong alignment of {110} ⟨001⟩ grains with respect to its RD. In the demagnetised state, antiparallel bar domains, with 180° walls, oriented along ⟨001⟩ grain axes are present throughout most of the material.

Widening or narrowing of adjacent domains under the influence of an external field applied parallel to the RD causes a dominant component of magnetisation along the RD. If the applied field is parallel to the RD, the resultant surface field and internal flux density are also parallel to the RD in a perfectly oriented Goss grain. When grains are misaligned from the RD, the situation can become very complex, especially if the applied field is at an angle to the RD.

Consider two identical hypothetical grains misaligned from the RD of a sheet of GOES by angles $\pm\alpha$. Suppose they each contain four bar domains and an external field $\boldsymbol{H_{ex}}$ is applied along the RD as shown schematically in Fig. 1(a). (Red and green arrows indicate the opposite magnetisation directions in adjacent domains). Angles of dip and roll are assumed to be negligible and closure domains are not included in this simple analysis.

The flux density out of each grain is $\boldsymbol{B}$ and the magnetisation is $\boldsymbol{M}$, so a demagnetising field $\boldsymbol{H_d}$ is set up in grain $\boldsymbol{m}$ as shown in Fig. 1(b). The resultant surface magnetic field strength $\boldsymbol{H}$ and $\boldsymbol{M}$ are not collinear and neither of them is parallel to the RD.

If $\boldsymbol{H_{ex}}$ is alternating in direction, it causes a loss in grain $\boldsymbol{m}$ which can be expressed as the sum of two components, one is a function of $\frac{dB\cos\hat{I}\pm}{dt}$

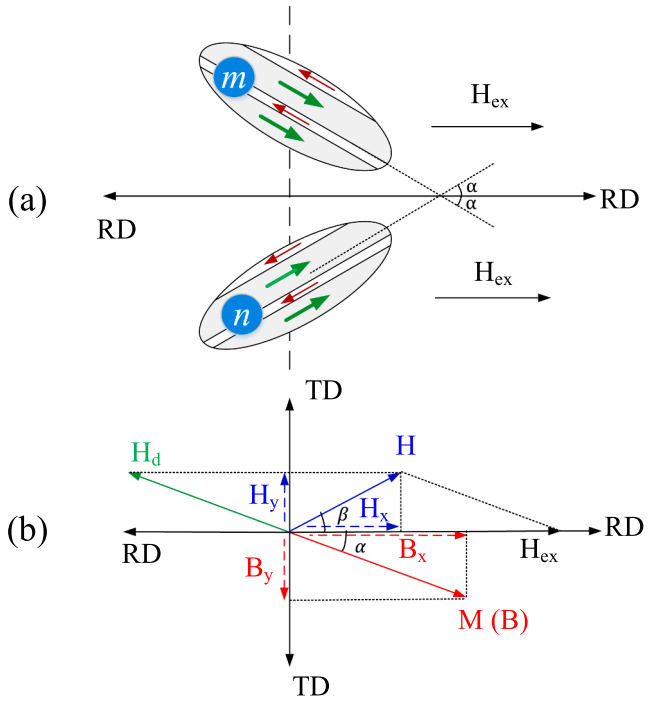

Fig. 1. (a) Schematic diagram of a simplistic domain structure in identical mis-oriented grains in a strip of GOES magnetised parallel to its RD. (b) Corresponding directions of magnetisation vectors in grain $\boldsymbol{m}$ (not to scale).

and $\boldsymbol{H}cos\beta$, and would be detected in an Epstein Square or a SST, and the other is a function of $\frac{dBsin\hat{i}\pm}{dt}$ and $\boldsymbol{H}sin\beta$. We refer to this second component as the transverse loss which neither an Epstein Square nor a SST would normally detect. The transverse loss[1] has been shown to account for more than 15% of the total loss in a sheet comprising poorly oriented Goss grains with a large size range [6]. This investigation is partly aimed at showing the extent to which the phenomenon can occur in commercial GOES where it is expected to be far lower.

3. Measurement system

3.1. Some considerations in design of the modified RSST

Although the RSST is mainly designed for testing under rotational magnetisation conditions, it is well suited for carrying out transverse flux measurements under unidirectional magnetisation at angles to the RD. The most important considerations in the measurement system topology are the sample shape and size, the magnetisation conditions and the $\boldsymbol{B}$ and $\boldsymbol{H}$ sensing methods. The main challenge is to accurately measure small directional variations of field and flux density which are highly dependent on the localised grain structure in the measurement region.

Orthogonal Rogowski-Chattock H-coils and B-coils can be used to measure components of $\boldsymbol{H}$ and $\boldsymbol{B}$ respectively in a strip sample [7]. However, drilling holes for search coils can degrade the local magnetic properties of the sample and several samples would be needed with the axes of orthogonal coils precisely located at specific angles to the RD making the arrangement difficult to produce accurately and time consuming to use. Holes can be avoided by using orthogonal needle probes to detect components of flux density [6].

Cross-stacked strip samples have been used to reduce demagnetising effects caused by shape anisotropy [8,9] but many samples cut at various angles to the RD are needed. Measuring local magnetisation conditions in the central region of a circular sample avoids the need to take account of this.

The currents in orthogonal magnetising windings can be controlled to set up unidirectional $\boldsymbol{B}$ as in [10,11]. Further details of conventional two-phase RSSTs are given in [10–12].

Based on the above considerations, and the authors' previous experience, it was decided to design a system based on a conventional two-phase RSST topology in which a circular sample could be rotated so that it could be uniaxially magnetised along any direction using just one magnetising winding. It was decided to use needle probes and H-coils for spacial average flux density and surface field measurements respectively. Their transverse components could be measured accurately enough to be able to confidently verify the presence of transverse loss less than 1% of the value of the total loss in GOES.

3.2. The modified RSST measurement system

The Modified RSST is shown in Fig. 2. A two-phase magnetising winding was incorporated so that measurements under rotational magnetisation could be carried out if required. In this investigation, only one magnetising winding, shown in red in Fig. 3 and designated as the (x) phase winding, was used. It sets up a unidirectional field along the (x) direction. The rotational stage enables the angular position of the sample to be set to an accuracy better than $\pm 1^\circ$ with respect to the magnetising coil axis.

[1] Transverse loss in this context is the portion of the total loss calculated from the components of field and flux density in the plane of a sheet at 90° to the direction of the applied magnetic field H_{ex}. This should not be confused with the loss occurring when GOES is magnetised along its TD, i.e. at 90° to the RD. To avoid any confusion, we generally refer to (x) and (y) directions being along, and at, 90° to the magnetising direction respectively.

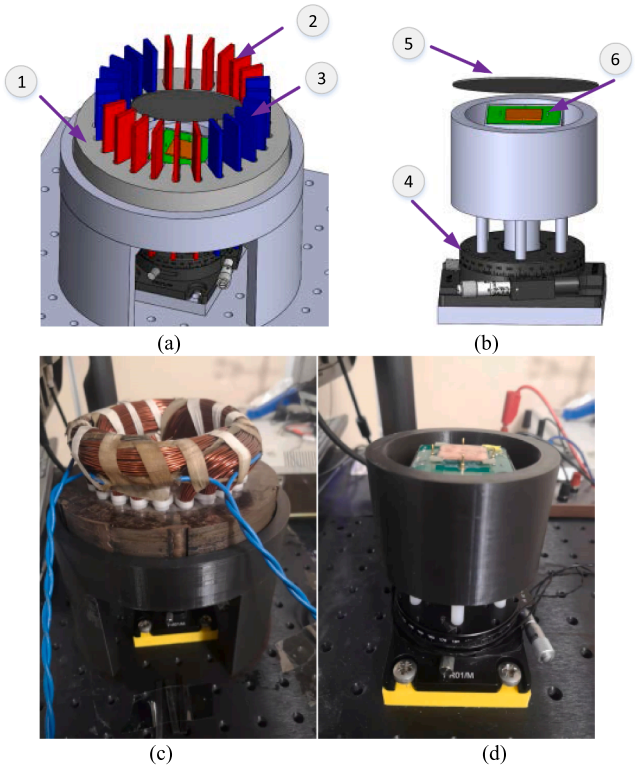

Fig. 2. The modified RSST (a) Complete system (b) Inner rotation stage (c) Photograph of the complete system (d) Photograph of the rotation stage. 1 Magnetising yoke. 2 (x) direction magnetising winding. 3 Un-energised (y) direction magnetising winding. 4 Angular adjustment. 5 Circular sample. 6 B-H sensor.

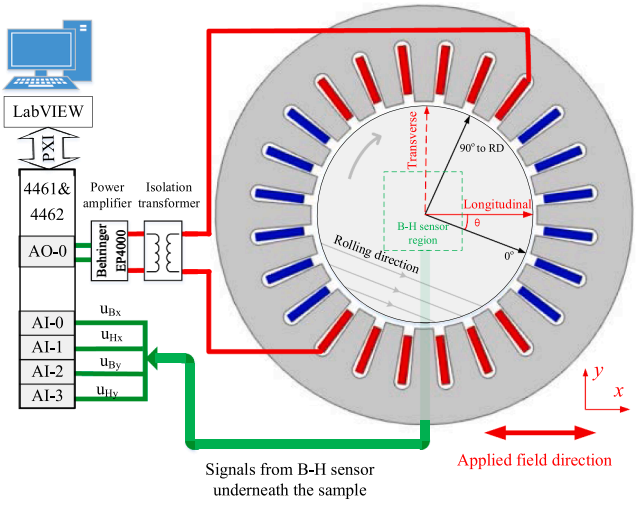

Fig. 3. Schematic diagram of the magnetising and measurement system showing a GOES sample oriented at an angle θ to the longitudinal (x) direction of the magnetising system.

Longitudinal and transverse components of the surface magnetic field and internal flux density were obtained using a vector B-H sensor, comprising orthogonal H-coils, located beneath the sample, and needle probes to measure the corresponding components of flux density. A 2 mm air gap between the 80 mm diameter sample and the magnetising yoke ensured that the magnetic field was uniform in the measurement region.

The measurement system uses LabVIEW controlled software, two 24-

bit National Instruments PXI-4461 & 4462 acquisition cards, a power amplifier and an isolation transformer as shown in Fig. 3. The maximum resolution of the data acquisition cards is 3.8×10^{-8} V, which ensures that the small transverse signals can be sampled accurately. The digital feedback algorithm described in [13] was used to obtain a controlled sinusoidal induction along the (x) direction (i.e. the longitudinal direction).

4. Measurement of Field Quantities and Loss

The B-H sensor on which the needle probes and H-coils were mounted is shown schematically in Fig. 4. Spring-loaded, 0.8 mm diameter, copper B-needles are welded into holes in the printed circuit board (PCB) so their tips made firm contact with the sample surface. The 200-turn H-coils were manufactured from 0.04 mm diameter copper wire wound around 0.4 mm thick plastic formers and securely fixed onto the PCB to sense H_x and H_y over a 30 mm × 30 mm measurement area. No correction was necessary to compensate for the different distances of the H-coils from the sample surface [14].

The flux density components were calculated from Eq. (1) in which d is the sample thickness and b is the distance between each pair of needles. V_{bx} and V_{by} are the instantaneous induced voltages measured across each pair of needles.

The H components were calculated using Eq. (2), in which μ_0 is the magnetic constant. The coil constants K_{hx} and K_{hy} were measured in a uniformly wound long solenoid. V_{hx} and V_{hy} are the instantaneous induced voltages across each coil. It should be noted that, the longitudinal direction (i.e. the direction of the applied field, $\boldsymbol{H_{ex}}$) is coincident with the (x) axis while the transverse direction is along the (y) axis. Thus, B_x, B_y and H_x, H_y are the instantaneous values of longitudinal and transverse components of $\boldsymbol{B}$ and $\boldsymbol{H}$.

$$\begin{cases} B_x = \dfrac{2}{bd}\int V_{bx}\,dt \\ B_y = \dfrac{2}{bd}\int V_{by}\,dt \end{cases} \tag{1}$$

$$\begin{cases} H_x = \dfrac{1}{\mu_0 K_{hx}}\int V_{hx}\,dt \\ H_y = \dfrac{1}{\mu_0 K_{hy}}\int V_{hy}\,dt \end{cases} \tag{2}$$

Based on Poynting's theorem, the total loss P_t can be expressed as the sum of the two components, P_x and P_y given in Eq. (3) where T is the time period of the alternating excitation and ρ the sample density. Although P_x and P_y are not physical quantities, we refer to them as the longitudinal and transverse components of loss respectively.

$$\begin{cases} P_x = \dfrac{1}{T\rho}\displaystyle\int_0^T H_x \frac{dB_x}{dt}dt \\ P_y = \dfrac{1}{T\rho}\displaystyle\int_0^T H_y \frac{dB_y}{dt}dt \\ P_t = P_x + P_y \end{cases} \tag{3}$$

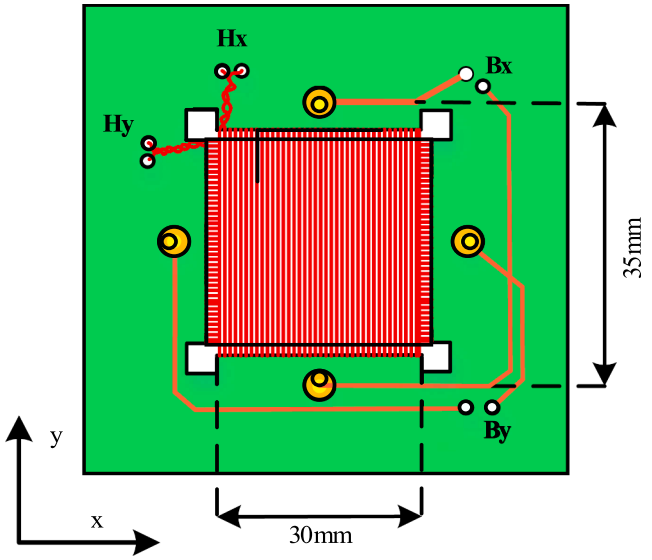

Fig. 4. Schematic of the vector B-H sensor.

5. Results

A 0.23 mm thick, 80 mm diameter, circular sample of GOES, was selected. Its static surface domain structure was observed using a magnetic domain viewer. Fig. 5 shows a schematic representation of the positions of the most prominent anti-parallel bar domains separated by 180° walls observed in the three well-oriented grains which occupy almost 80 % of the measurement area. The ⟨001⟩ axes of grains i and k were within 1° of the RD and grain j, extending over about 40% of the region, had a yaw angle of approximately 5°. The position of the Bloch walls were within 5 μm of each other on either side of the sample.

The sample was inserted into the Modified RSST and. magnetised by a unidirectional, alternating field at angles between −90° and +90° to the RD. The plus and minus designations refer to magnetisation being along equivalent directions on either side of the RD where a positive angle refers to a clockwise rotation with respect to Fig. 3. For each magnetisation direction, B-H measurements were made under peak sinusoidal inductions from 0.5 T to 1.7 T at 0.2 T intervals. Measurements were performed at 20 Hz since both the signal to noise ratio of the transverse components of B and H and the classical eddy current loss were low at this frequency.

Longitudinal (x) and transverse (y) field and flux density components were recorded and the corresponding loss components were calculated based on the formulations in Eq. (3). In the following, B_{xp} (B_{yp}) and B_{xrms} (B_{yrms}) represent the amplitude and root-mean-square (rms) of the components of flux density respectively. The same notation is applied to the field components.

5.1. Assessment of the repeatability

To verify that no artefacts of the measurement system were causing any systematic error, a series of measurements were made with the specimen placed in different positions in the apparatus. It was

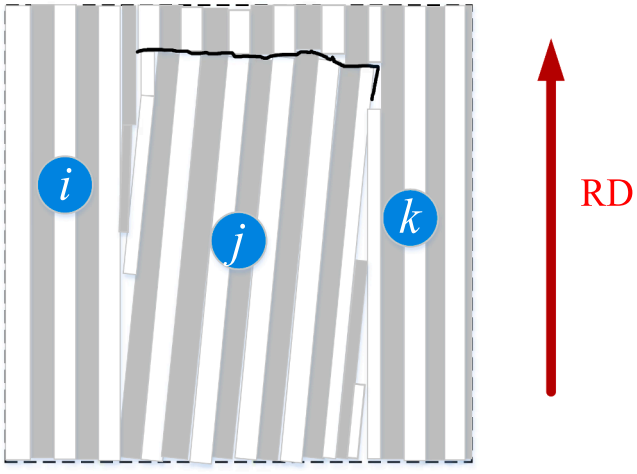

Fig. 5. Schematic diagram of grain and domain structure in the measurement area.

magnetised at 45° to the RD at 1.5 T and measurements were repeated after rotating the sample through 180° and again after turning it over. The values of B_{xrms} agreed to within 0.5% while the much lower B_y measurements differed by less than 6 %. The corresponding values of H_{xrms} and H_y were within similar ranges. These results confirmed that the Modified RSST was capable of accurately recording the variation of B_y and H_y with magnetising angle.

While magnetised at 30° to the RD at 1.5 T, a similar series of measurements were repeated three times before and after the specimen was removed and replaced in the apparatus. The relative standard deviation of longitudinal and transverse loss components were 1.5% and 3.0%, respectively.

5.2. Longitudinal B-H loops and magnetisation curves

Fig. 6 shows longitudinal magnetisation curves when the magnetising field was applied at angles between 0° and +90° to the RD. Below 1.1 T, the TD was the hardest direction of magnetisation but the hard direction shifted to 55° to the RD at higher flux densities which is consistent with several previous findings (e.g. [18–20]). An influence of increasing [100] or [010] domain activity on magnetisation at angles higher than 30° to the RD was also apparent.

5.3. Analysis of magnetisation components

Longitudinal and transverse components of magnetic field and flux density, at different magnetising directions are presented in Fig. 7. Fig. 7 (a) shows the sinusoidally controlled B_x waveforms of 1.3 T amplitude along five magnetising directions. The magnitudes of the transverse B_y components in Fig. 7(b), are all less than 1.5% of the corresponding B_x values. When magnetised along the RD, B_y is in phase with B_x and sinusoidal but, for all other magnetising directions, it becomes non-sinusoidal and the degree of distortion varies with magnetisation angle. The transverse H_y components are much more pronounced than B_y when compared with their counterparts along the longitudinal direction because the permeability is lower when magnetised along these directions due to the difficulty of moving domains away from [100] and [010] directions.

The time-domain waveforms of H_x, B_y and H_y are markedly non-sinusoidal at high applied fields. Their rms characteristics shown in Fig. 8 illustrate their behaviour more clearly. Fig. 8(a) shows that the longitudinal magnetic flux densities are well controlled under each magnetisation condition. Fig. 8(c) shows that the hardest direction of magnetisation was at around 70° to the RD at low flux density and gradually reduces to 50° at high values of B_{xrms}.

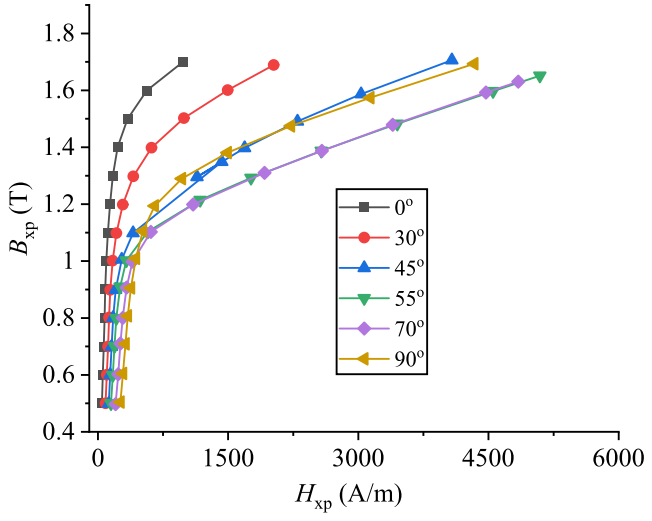

Fig. 6. Longitudinal magnetisation curves measured when magnetised at 20 Hz along directions between 0° and +90° to the RD.

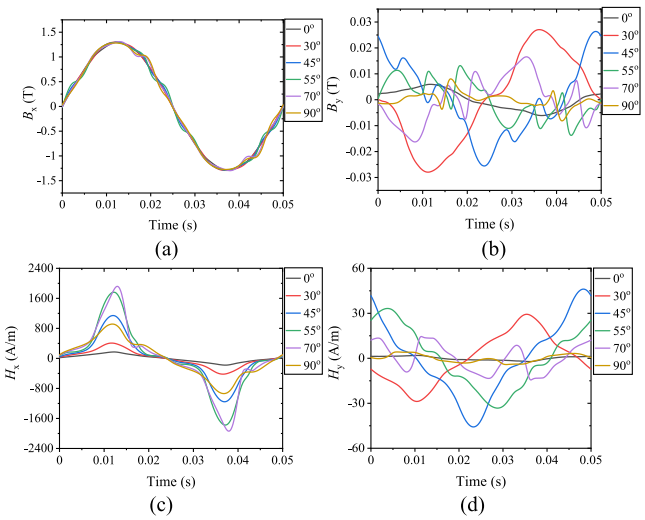

Fig. 7. Waveforms of components of magnetic field strength and flux density over one cycle of magnetisation measured when magnetised along different directions at 20 Hz and B_{xp} = 1.3 T (a) B_x (b) B_y (c) H_x (d) H_y.

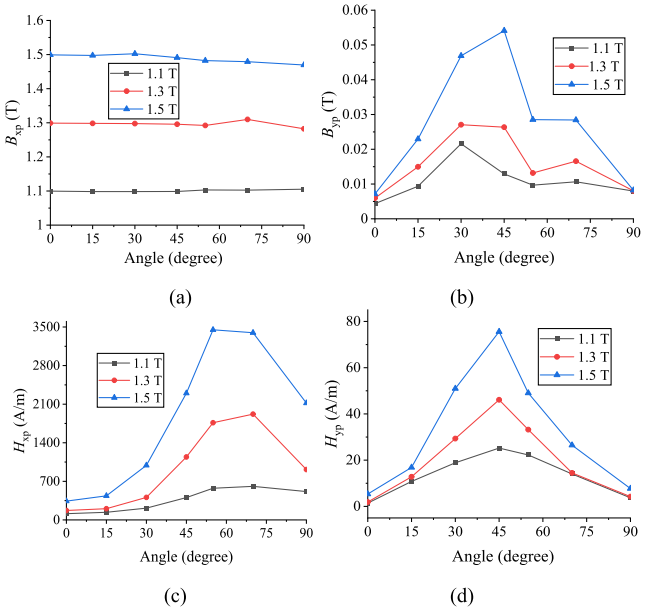

Fig. 8. Calculated rms values of magnetic flux density and field components when magnetised along different directions at 20 Hz. (a) B_{xp} (b) B_{yp} (c) H_{xp} (d) H_{yp}.

H_{yrms} always reaches a maximum at a magnetisation angle of approximately 45° to the RD as illustrated in Fig. 8(d). The angular variation of B_{yrms} shown in Fig. 8(b) is more irregular than that of B_{xrms} simply because B_x was forced to be sinusoidal whereas the magnitude of B_y depends on the permeability along the direction at 90° to the field direction. The reason for the decrease in the transverse flux density above 45° to the RD and at high inductions is unclear but is related to the complex evolution of magnetic domains when the sample is subjected to large unidirectional applied fields along difficult magnetisation directions. However, in all cases, it can be seen that the magnitudes of both transverse components, B_{yrms} and H_{yrms}, are largest when the sample is magnetised along directions other than at either 0° or 90° to the RD although neither are more than around 7% of the corresponding

longitudinal values under any magnetisation conditions.

5.4. Loss components

Fig. 9 shows the variation of the longitudinal component of loss P_x and the transverse component P_y in the sample magnetised uniaxially along four directions at 20 Hz. A component of transverse loss is always present. Although far smaller, it follows the same trend as P_x. When magnetised along the RD or the TD, it is negligible. It rises to no more than 1.0% of the total loss when magnetised along any other direction.

The angular dependence of the loss components is shown in Fig. 10. The magnetisation angle at which the highest longitudinal loss P_x occurred, was between 55° and 70° to the RD. It slightly shifts towards the RD as the flux density increases. This is related to the shift in the hard magnetising direction mentioned in Section 5.2. The directional characteristic of P_y, seen in Fig. 10(b), is different to that of P_x. However, the fact that they are similar when magnetised along positive or negative angles with respect to the RD shows that this is due to the effect of the local grain structure rather than random, systematic errors which could be significant at low magnetisation levels.

The variation of the proportion of transverse loss in the total loss with excitation direction and induction level is shown in Fig. 11 for positive angles of magnetisation with respect to the RD. The P_y/P_t ratio is dependent on the direction in which the field was rotated, so a slightly more representative value would be obtained by averaging results from clockwise and anticlockwise rotation. However, there is no practical benefit in doing so since the results were characteristic of a few grains in the measurement region which may not be representative of a larger volume of steel.

The ratio, P_y/P_t, reached a peak when magnetised along a direction between 30° and 45° to the RD. The dependence of the loss components on the magnetisation direction at low angles to the RD is shown in Fig. 12. In this region, the simple model given in Fig. 1 is expected to be applicable to show the reason for the asymmetry of the characteristics with respect to the RD. The loss components were consistently highest when magnetised at negative angles to the RD, i.e. when the sample was rotated in a clockwise direction.

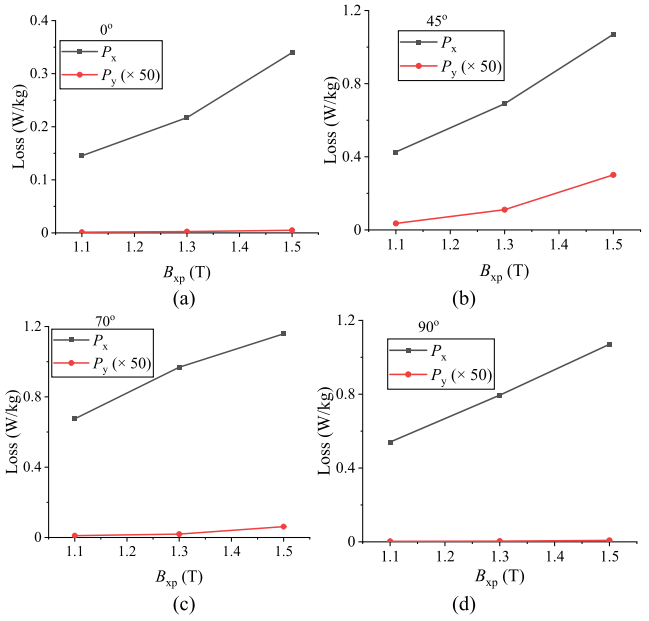

Fig. 9. Variation of measured longitudinal loss P_x, transverse loss P_y and total loss P_t with B_{xp} between 1.1 T and 1.5 T magnetised at (a) 0°, (b) +45°, (c) +70°, (d) +90°, to the RD. Note the P_y characteristic is magnified by a factor of 50.

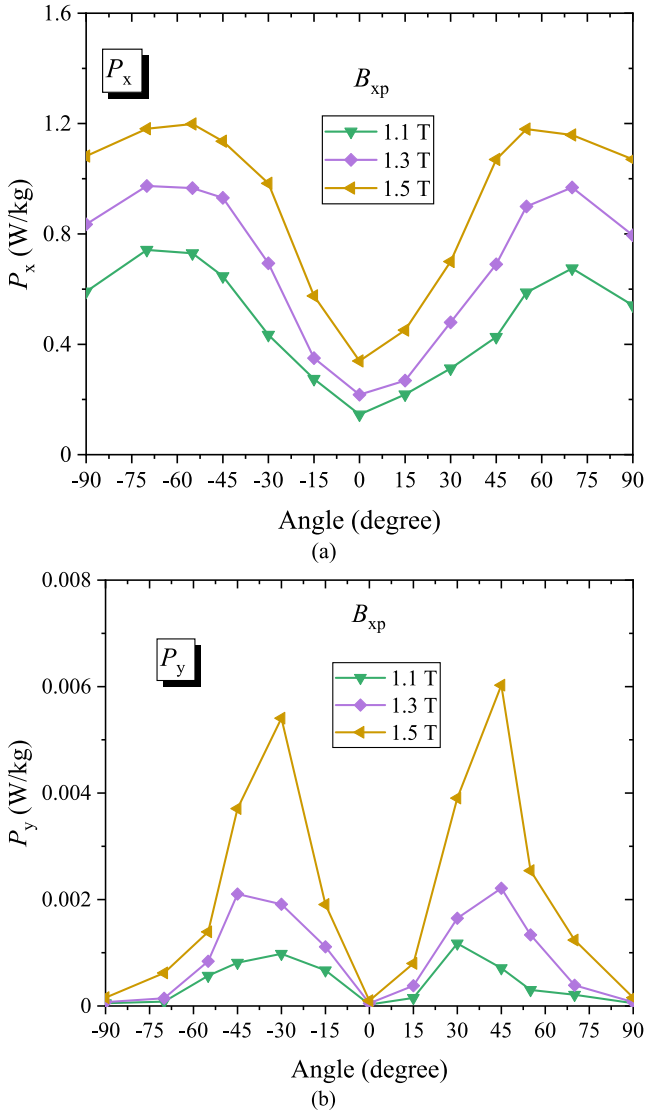

Fig. 10. Components of measured loss in the sample magnetised at angles between 0° and ±90° to the RD at B_{xp} between 1.1 T and 1.5 T. (a) Longitudinal loss P_x, (b) Transverse loss P_y.

6. Discussion

It has been realised for many years that the field on the surface of magnetised GOES varies in magnitude and direction dependent on the local grain structure. Vector *B-H* scanners are used to detect orthogonal components of ***B*** and ***H*** from which the local loss can be obtained using forms of Eq. (3). Results obtained from many studies have shown significant deviation of the local field from both the RD and ⟨001⟩ directions of mis-oriented grains but the occurrence of transverse magnetisation and loss has not been widely recognised.

The non-symmetry of the loss characteristics in Figs. 10 and 12 has not been reported previously. It is dependent on the grain and domain structures in the measurement region. It can be deduced from Fig. 1(b) that, if an external field is applied along the RD, no transverse loss should be produced in Grains *i* and *k* but a component of transverse flux in Grain *j* generates transverse loss in that grain according to Eq. (3).

Suppose the sample is rotated 5° in an anticlockwise direction, then the ⟨001⟩ directions of Grains *i* and *k* will be at 5° to the applied field and that of Grain *j* will be along the field direction. Since the grains are similar in size, the total transverse loss should be about the same as when magnetised along the RD. However, if the sample is rotated by 5°

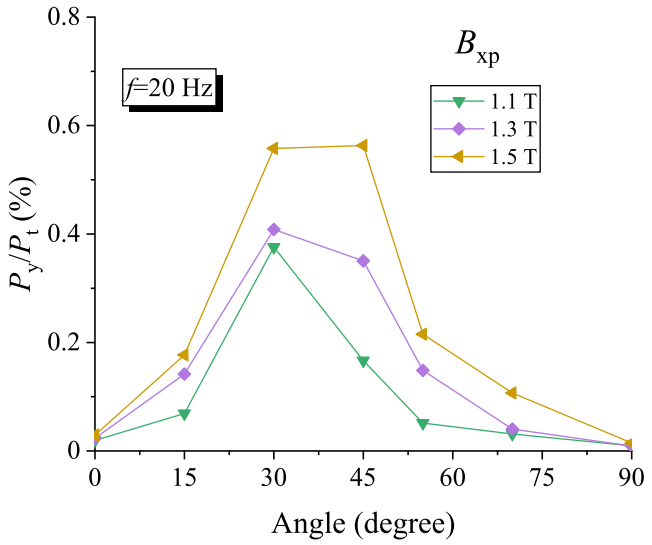

Fig. 11. The magnetisation direction dependence of the percentage of transverse loss in the total loss.

in the clockwise direction, the [001] directions in Grains *i* and *k* will be at 5°, and that of Grain *j* will be at 10°, to the applied field direction.

Hence transverse loss will occur in all grains and its total value is higher than when the magnetisation is rotated by the same amount in the opposite direction. The difference increases significantly if the field is applied at higher angles to the RD.

The average mis-orientation in the measurement region was approximately 5° and the transverse loss was close to zero when magnetised at between +3° and +5° to the RD. Based on the simple model in Fig. 1, and the fact that no grains oriented at negative angles to the RD were observed in the measurement region, we would expect the transverse loss to be zero when the sample was magnetised 5° to the RD The agreement is not very good because the presence of some smaller grains, whose orientations and domain structures were uncertain, was not accounted for in this simple analysis. Also, it is likely that the flux density in grains *j* was lower than in the well-oriented grains. If this is so, the transverse loss would fall to zero when H_{ex} was applied along a direction closer to the RD.

It is interesting to note that the low angle characteristics shown in Fig. 12 fit the relationship $P_y \propto \sin^2\theta$ but it breaks down completely when magnetised at higher angles to the RD as seen in Fig. 10.

Fuller detail of the microstructure and the static domain structure is needed to obtain a more accurate quantification of the relationship between magnetisation angle and transverse loss in GOES. It would be useful to carry out measurements on a (110) ⟨001⟩ oriented single crystal of 3%SiFe to minimise the number of assumptions which have to be made in any analysis. This would also eliminate any magnetic interaction between adjacent grains affecting the transverse magnetisation.

The loss due to transverse magnetisation reported here is no more than 1% of the total loss. This is far lower than earlier reports. For example, the local transverse loss up to 15% of the total loss reported in [6] was measured in a sheet of GOES with a wide spread of grain sizes and large mis-orientation angles which caused high transverse magnetisation [22]. The local transverse flux in a laboratory prepared strip of large grain, highly mis-oriented steel, was found to be up to around 30% of the longitudinal value [23].

Although the results show that transverse loss is negligible in well oriented GOES it should be noted it is possible that it could become more significant under highly distorted flux conditions.

Computational electromagnetic solvers do not take account of grain and domain structures which have large effects on localised

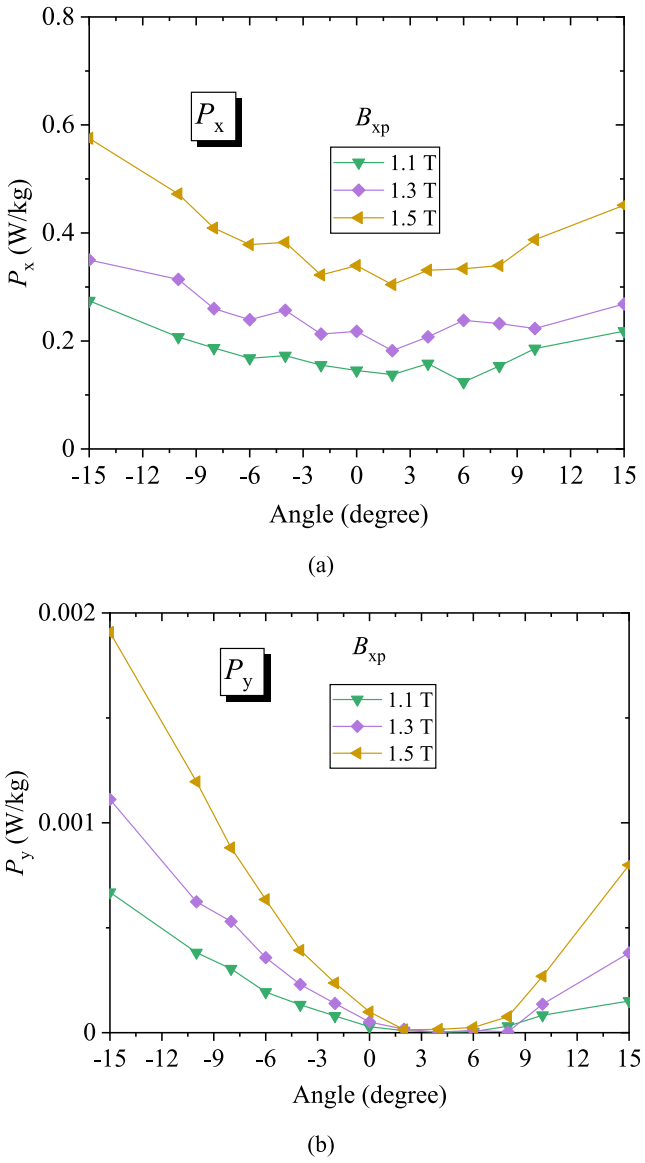

Fig. 12. Variation of loss components with magnetisation direction at low angles to the RD, (a) P_x and (b) P_y.

magnetisation conditions but it appears that ignoring their effect on transverse flux in regions of GOES cores where magnetisation is not along the RD of the steel is of no consequence.

Likewise, it can be estimated from the results here that transverse loss accounts for less than 0.1% of the BFs of energy efficient transformer cores so there is no advantage in including it separately in BF prediction algorithms.

The loss measured using IEC Standard methods will always be a little lower than the absolute value because they do not account for transverse magnetisation but under normal circumstances the error is negligible.

Although the magnetisation sensors are sufficiently accurate to measure transverse loss, the results are highly dependent on the sensor size. If the measurement area is too small, the *B* and ***H*** signals will be inaccurate and, if too large, localised transverse flux components will cancel out so the transverse loss may be grossly underestimated. The transverse loss is expected to be highest in less well oriented grades of steel but fortunately it is still not likely to be large enough to have any impact on the commercial grading of loss in GOES.

It remains to be seen whether transverse loss is of any significance in the presence of mechanical stress or under rotational or complex

magnetisation conditions.

The Modified RSST was used to look for evidence of transverse flux in a 0.35 mm thick, NO electrical steel whose loss anisotropy factor was 10%. Transverse magnetisation appeared to follow similar trends with magnetisation direction to that of GOES despite the far different microstructure and domain distribution. However, the conventional sensors used in this investigation were too large to measure the true transverse magnetisation in such small grains so no results are presented here.

7. Conclusions

The following conclusions can be drawn

- The uncertainty level of *B-H* characteristics and losses measured using a Modified RSST was sufficiently low for it to be confidently used to investigate transverse magnetisation phenomenon in electrical steel.
- Transverse magnetisation is responsible for up to around 1% of the total loss in well oriented GOES depending on the magnetisation direction.
- A simple magnetic domain model is sufficient to demonstrate the origin of transverse loss in mis-oriented grains.
- Under normal circumstances, transverse magnetisation in GOES can be ignored in computational electromagnetic field solvers, transformer BF calculations and in commercial loss grading of GOES.
- Low levels of transverse magnetisation appears to occur in NO electrical steel but it is difficult to quantify.

CRediT authorship contribution statement

Shuaichao Yue: Investigation, Formal analysis, Writing – review & editing. **Anthony J. Moses:** Conceptualization, Writing – original draft, Data curation, Writing – review & editing. **Philip I. Anderson:** Writing – review & editing, Funding acquisition. **Christopher Harrison:** Software, Writing – review & editing. **Yongjian Li:** Supervision. **Qingxin Yang:** Supervision.

Declaration of Competing Interest

The authors declare that they have no known competing financial interests or personal relationships that could have appeared to influence the work reported in this paper.

References

[1] A. Moses, P. Anderson, K. Jenkins, H. Stanbury, Electrical Steels Volume 1: Fundamentals and Basic Concepts, Inst. Eng. Technol. (2019) 316–319.
[2] A.J. Moses, Prediction of core losses of three phase transformers from estimation of the components contributing to the building factor, J. Magn. Mag. Mat. 254 (2003) 615–617.
[3] Y. Guo, J.G. Zhu, J. Zhong, H. Lu, J.X. Jin, Measurement and modeling of rotational core losses of soft magnetic materials used in electrical machines: a review, IEEE Trans. Magn. 44 (2) (2008) 279–291.
[4] S. Yue, Y. Li, Q. Yang, K. Zhang, C. Zhang, Comprehensive investigation of magnetic properties for Fe–Si steel under alternating and rotational magnetizations up to kilohertz range, IEEE Trans. Magn. 55 (7) (2019) 1–5.
[5] N. Takahashi, Y. Mori, Y. Yunoki, D. Miyagi, M. Nakano, Development of the 2-D single-sheet tester using diagonal exciting coil and the measurement of magnetic properties of grain-oriented electrical steel sheet, IEEE Trans. Magn. 47 (10) (2011) 4348–4351.
[6] A.J. Moses, S.N. Konadu, S. Zurek, Losses due to the transverse component of flux density in grain oriented electrical steels, J. Optoelectron. Adv. Mater. 10 (5) (2008) 1110.
[7] O. Benda, J. Bydzovský, E. Ušák, Combined influence of shape and magnetocrystalline anisotropy on measured magnetisation curves of SiFe sheets, Le J. Phys. IV 8(PR2) (1998) Pr2-627-Pr2-630.
[8] F. Fiorillo, L. Dupré, C. Appino, A. Rietto, Comprehensive model of magnetization curve, hysteresis loops, and losses in any direction in grain-oriented Fe-Si, IEEE Trans. Magn. 38 (3) (2002) 1467–1476.
[9] O. Bíró et al., Analytical model for magnetic anisotropy of non-oriented steel sheets, COMPEL: Int. J. Comput. Math. Electr. Electron. Eng. (2015).
[10] Y. Tamura, Y. Ishihara, T. Todaka, Measurement of magnetic characteristics of silicon steel in any direction by RSST and SST: method and relationship, J. Magn. Mag. Mat. 133 (1–3) (1994) 382–385.
[11] G. Bavendiek, N. Leuning, F. Müller, B. Schauerte, A. Thul, K. Hameyer, Magnetic anisotropy under arbitrary excitation in finite element models, Arch. Electr. Eng. 68(2) (2019).
[12] S. Zurek, Characterisation of Soft Magnetic Materials Under Rotational Magnetisation, CRC Press, 2017.
[13] C.W. Harrison, P.I. Anderson, Characterization of grain-oriented electrical steels under high DC biased conditions, IEEE Trans. Magn. 52 (5) (2016) 1–4.
[14] F. Fiorillo, Measurement and Characterization of Magnetic Materials, North-Holland, 2004.
[18] K. Chwastek, A. Baghel, M. De Campos, S. Kulkarni, J. Szczygłowski, A description for the anisotropy of magnetic properties of grain-oriented steels, IEEE Trans. Magn. 51 (12) (2015) 1–5.
[19] C. Appino, E. Ferrara, F. Fiorillo, C. Ragusa, O. de la Barrière, Static and dynamic energy losses along different directions in GO steel sheets, J. Magn. Mag. Mat. 500 (2020) 166281.
[20] W.A. Pluta, Angular properties of specific total loss components under axial magnetization in grain-oriented electrical steel, IEEE Trans. Magn. 52 (4) (2015) 1–12.
[22] S.N. Konadu, Non-destructive testing and surface evaluation of electrical steel, PhD Thesis, Cardiff University, May, 2006.
[23] X.T. Xu, Localised variation of magnetic properties of grain oriented electrcal steels, PhD Thesis, Cardiff University, July, 2014.